AFD Thermosensory Neurons Mediate Tactile-Dependent Locomotion Modulation in *C. elegans*

Manuel Rosero[1,2] and Jihong Bai[1,2,#]

[1] Basic Sciences Division, Fred Hutchinson Cancer Center, Seattle, WA 98109

[2] Molecular and Cellular Biology Graduate Program, University of Washington, Seattle, WA 98109

[#] Jihong Bai, Ph.D. (Corresponding author)
Basic Sciences Division
Fred Hutchinson Cancer Center
1100 Fairview Ave N.
Seattle, WA 98109, USA
Email: jbai@fredhutch.org

ABSTRACT

Sensory neurons drive animal behaviors by detecting environmental stimuli and relaying information to downstream circuits. Beyond their primary roles in sensing, these neurons often form additional synaptic connections outside their main sensory modality, suggesting broader contributions to behavior modulation. Here, we uncover an unexpected role for the thermosensory neuron AFD in coupling tactile experience to locomotion modulation in *Caenorhabditis elegans*. We show that while AFD employs cGMP signaling for both thermotaxis and tactile-dependent modulation, the specific molecular components of the cGMP pathway differ between these two processes. Interestingly, disrupting the dendritic sensory apparatus of AFD, which is essential for thermotaxis, does not impair tactile-based locomotion modulation, indicating that AFD can mediate tactile-dependent behavior independently of its thermosensory apparatus. In contrast, ablating the AFD neuron eliminates tactile-dependent modulation, pointing to an essential role for AFD itself, rather than its sensory dendritic endings. Further, we find tactile-dependent modulation requires the AIB interneuron, which connects AFD to touch circuits via electrical synapses. Removing innexins expressed in AFD and AIB abolishes this modulation, while re-establishing AFD-AIB connections with engineered electrical synapses restores it. Collectively, these findings uncover a previously unrecognized function of AFD beyond thermosensation, highlighting its influence on context-dependent neuroplasticity and behavioral modulation through broader circuit connectivity.

INTRODUCTION

Adaptive behavioral responses require animals to interpret sensory signals in the context of prior experiences, enabling effective responses to changing environmental conditions. For example, rodents associate contextual cues, such as odors and colors, with rewards or punishments, leading to context-dependent adjustments in approach or avoidance behaviors [1,2]. Disruptions in the biological processes underlying this plasticity, as seen in neurological and psychiatric disorders, often result in impaired behavior modulation based on prior sensory experiences [3–7]. Recognizing the critical role of context-dependent behavioral modulation for survival and well-being, ongoing research focuses on uncovering the neuroplastic mechanisms responsible for these adaptive processes.

Studies across diverse organisms reveal that animals, regardless of nervous system complexity, integrate prior sensory experiences to shape behavior [8–15]. In the nematode *C. elegans*, which has only 302 neurons, locomotion strategies are modified by prior exposure to stimuli such as odors, touch, light, and starvation, demonstrating robust adaptive behaviors [16–23]. The wide range of adaptive behaviors, combined with the well-mapped *C. elegans* nervous system and abundant genetic tools, have empowered the discovery of fundamental circuit mechanisms and molecular pathways underlying context-dependent behavioral modulation [24–28].

The *C. elegans* sensory system comprises 60 ciliated sensory neurons specialized in detecting chemical, thermal, mechanical, and olfactory stimuli [29,30]. Each sensory neuron has a dendritic apparatus that converts specific environmental signals into neuronal activity, which drives signal flow through downstream networks of interneurons and motor neurons, ultimately shaping behavior [31–33]. Among these, AFD, a pair of bilaterally symmetric left-right neurons, serves as the primary thermosensory neurons required for thermotaxis (movement toward the a preferred temperature) [34]. The dendritic endings of AFD, enriched with microvilli, serve as the primary site for thermal detection. Even when detached from the cell body, these dendritic endings retain calcium responsiveness to temperature stimuli [35]. Moreover, genetically disrupting these sensory endings abolishes the Ca^{2+} response in AFD cell bodies to temperature changes and eliminates thermotaxis, underscoring their essential role in thermal sensing [36–38].

The second messenger cyclic guanosine monophosphate (cGMP) plays a central role in modulating AFD thermosensory activity. Temperature changes in AFD neurons trigger intracellular Ca^{2+} dynamics, with Ca^{2+} levels rising during warming and falling during cooling [35,39,40]. This response relies on cGMP synthesis mediated by the guanylyl cyclases (GCs) *gcy-8*, *gcy-18*, and *gcy-23*, which have overlapping but distinct roles. Specifically, *gcy-8* is essential for generating thermally evoked Ca^{2+} responses in AFD [41,42], whereas *gcy-18* and *gcy-23* act synergistically to sustain temperature sensing [41,43]. The cGMP produced by these cyclases activates cyclic nucleotide-gated (CNG) channels, comprised of alpha-subunits TAX-4 and beta-subunits TAX-2, resulting in increases in intracellular Ca^{2+}. Mutations in either *tax-4* or *tax-2* abolish thermally evoked Ca^{2+} responses in AFD and disrupt thermotaxis, underscoring the importance of cGMP signaling for AFD-mediated thermosensation [40].

AFD transmits thermal signals to several downstream interneurons, including AIY, AIZ, and AIB, which process this information to guide temperature-dependent behaviors. Thermotaxis in *C. elegans* encompasses three categories: movement toward warmer temperatures (thermophilic), movement toward cooler temperatures (cryophilic), and movement within a preferred temperature range (isothermal) [44,45]. Each behavior type depends on distinct AFD synaptic partners: AIY is critical for thermophilic and isothermal behaviors [46,47]; AIZ is specific for cryophilic behavior [48–50]; and AIB also supports thermophilic behavior, though its role is less critical than that of AIY [51]. These findings demonstrate the functional specificity of synaptic partners of AFD neurons in shaping distinct temperature-dependent behaviors.

In this study, we demonstrate that AFD plays a novel role in tactile-mediated, context-dependent locomotion modulation, thereby expanding its function beyond temperature sensing. The mechanisms underlying this role differ markedly from those involved in thermosensation. First, context-dependent modulation requires distinct cGMP signaling components. Second, while the microvilli-rich sensory endings of AFD are essential for thermosensation, they are dispensable for context-dependent modulation. Third, this modulation depends on mechanosensory neurons and on electrical synapses between AFD and the AIB interneuron, which connects to mechanosensory circuits. Finally, disruption of *inx-7* and *inx-10* genes, encoding gap junction protein innexins in AFD and AIB, impairs context-dependent locomotion modulation. Remarkably, restoring AFD–AIB connectivity via engineered Cx36 electrical synapses rescues this function.

Collectively, our findings uncover an unconventional mechanism by which AFD mediates behavior modulation based on tactile experience.

RESULTS

C. elegans displays distinct locomotion in identical environments after exploring different physical structures.

To investigate the impact of prior experience on *C. elegans* behavior, we first allowed worms to explore chambers with distinct pillar designs (exploration zone, Fig. 1A) before recording their locomotion in identical assay zones (red dashed-line boxes, Fig. 1A). We hypothesized that if behavior were solely driven by immediate sensory input, worms in identical assay zones would exhibit similar locomotion. Conversely, if prior experience, such as exposure to different physical features in the exploration zones, influences behavior, then worms should display distinct locomotor patterns even in the identical assay zones. To test these hypotheses, we employed two types of microfluidic chambers: uniform and binary (Fig. 1A). Both chamber types include an identical assay zone. Once worms enter this zone, their immediate environment is the same regardless of the chamber. However, before reaching the assay zone, worms explore surrounding areas with pillar designs that differ in size and spacing. This design allowed us to assess how prior exposure to different physical contexts impacts locomotion in an otherwise identical setting.

Worms were allowed to explore the chambers for 60 minutes before their behavior was recorded in the assay zones. We found that worms in the uniform chamber assay zone exhibited locomotor behavior that differed from that of worms in the binary chamber assay zone (Fig. 1B-F). Specifically, in the uniform chamber assay zone, worms moved approximately 40% faster (Fig. 1B, F), spent about 20% less time idle (Fig. 1C, F), reversed direction around 20% less frequently (Fig. 1D, F), and turned about 30% more often (Fig. 1E, F) than worms in the binary chamber assay zone. These findings demonstrate that locomotion adjustments are shaped by past sensory experience rather than solely by immediate environmental cues. That worms exhibited different behaviors in identical assay zones highlights the flexible, context-dependent nature of *C. elegans* behavior.

118 **Guanylyl cyclase gene *gcy-18* is required for context-dependent locomotion modulation in chambers.**

119 To identify mechanisms underlying context-dependent locomotion adjustments, we employed a
120 previously reported preference assay that uses microfluidic arenas to assess the ability of worms to select a
121 preferred space [52]. Because worms must adjust their locomotion based on their surroundings to remain
122 within a preferred area, we hypothesized that mutations abolishing this preference would reveal key
123 mechanisms underlying context-dependent adjustments in the uniform and binary chambers. Accordingly, we
124 screened for mutant worms that failed to choose their preferred area, aiming to identify the genetic
125 mechanisms mediating locomotion adjustments in response to different physical structures. Given the
126 significant role of cGMP in neuronal plasticity and behavior modulation, we performed a small-scale genetic
127 screen using loss-of-function mutants for 24 genes encoding guanylyl cyclase (GC), the enzyme responsible
128 for cGMP synthesis. Using the preference assay, we identified two putative null mutants, *gcy-18(gk423024)*
129 and *gcy-12(gk142661),* that failed to display a spatial preference (Supp Fig. 1). We then compared the
130 locomotion properties of *gcy-18* and *gcy-12* mutants in both uniform and binary chambers. Our results showed
131 that *gcy-18* mutants failed to execute context-dependent adjustments, displaying similar locomotion rates in
132 both chamber types. Specifically, *gcy-18* mutants exhibited a significantly reduced Δspeed ($3 \pm 5\%$) compared
133 to wild type ($35 \pm 7\%$, $p<0.001$, Fig. 2A). In contrast, *gcy-12* mutant worms exhibited normal speed adjustment,
134 with Δspeed values comparable to wild type (Fig. 2A). This indicates that *gcy-12* is not required for the
135 modulation of locomotion speed. In comparison, the failure of *gcy-18* mutants to adjust their speed suggests
136 that *gcy-18* plays a critical role in context-dependent behavioral adjustment. Together, these results
137 demonstrate that among the guanylyl cyclases, *gcy-18* is essential for the context-dependent modulation of
138 locomotion.

139 To confirm that the defects observed in *gcy-18* mutants were not due to background artifacts, we
140 introduced a single-copy transgene that drives *gcy-18* cDNA expression under the control of a *gcy-18* promoter
141 into *gcy-18(gk423024)* mutants to test whether reintroducing a functional copy of *gcy-18* could rescue the
142 behavioral defects. Indeed, expression of the transgene restored locomotion adjustments (Δspeed: $20 \pm 6\%$) to
143 levels closer to those observed in wild type animals ($35 \pm 7\%$, $p = 0.4$, Fig. 2B), confirming the crucial role of
144 *gcy-18* in mediating these adjustments based on the experience of exploring physical environments. The
145 identification of *gcy-18* was particularly intriguing, as its expression is restricted to a single pair of neurons, the

146 thermosensory AFDs. Given that our assay chambers lacked thermal gradients, this finding suggests a novel
147 role for *gcy-18* and AFD neurons in mediating locomotion adjustments in response to the exploration of
148 surrounding physical structures.

149 To further investigate the role of AFD-specific guanylyl cyclases in context-dependent locomotion
150 modulation, we examined *gcy-8*, which is essential for generating thermally evoked Ca^{2+} responses in AFD
151 [41,42]. In thermal responses, disrupting *gcy-8* alone is sufficient to impair AFD function, whereas disruption of
152 *gcy-18* alone does not [41,43], indicating the critical role of GCY-8 in AFD thermosensation. If *gcy-18*
153 influenced behavioral adjustment in microfluidic chambers solely through its role in thermosensation, we would
154 expect that a loss-of-function mutation in *gcy-8* would have a similar or even more disruptive impact on
155 locomotion modulation. However, *gcy-8* mutant worms exhibit little change in their ability to adjust locomotion
156 speed (Δspeed: 29 ± 7%), with Δspeed values similar to that observed in wild type worms ($p = 0.96$, Fig. 2C).
157 These results indicate that while *gcy-8* is critical for thermosensation, its mutation does not affect context-
158 dependent locomotion modulation, suggesting that independent cGMP signaling mechanisms govern AFD
159 neuronal activity in thermosensation and context-dependent behavior in microfluidic chambers (Fig. 2D).
160

161 **Distinct CNG channels mediate context-dependent locomotion modulation and thermosensation.**

162 The role of guanylyl cyclase in cGMP synthesis prompted us to investigate whether cyclic nucleotide-
163 gated (CNG) channels are involved in context-dependent locomotion modulation. CNG channels, composed of
164 α and β subunits, open upon binding cyclic nucleotides (*e.g.*, cGMP and cAMP), allowing Ca^{2+} influx [53–56] to
165 control signal transduction and neural plasticity across species [57–64] (Fig. 3A). In *C. elegans*, mutations in
166 either the *tax-4* or *tax-2* genes, which encode the α and β subunits of CNG channels respectively, impair
167 thermotaxis behavior [47,65] and disrupt AFD neuron responses to temperature changes [40,66]. To determine
168 their role in context-dependent locomotion modulation, we examined *tax-4(p678)* and *tax-2(p694)* mutant
169 worms using our microfluidic chamber assay.

170 We found that *tax*-2 is essential for context-dependent locomotion modulation, as *tax-2* mutants did not
171 exhibit differences in speed between chamber types (Fig. 3B, C). In contrast, *tax-4* mutants displayed an
172 enhanced locomotion adjustment compared to wild type worms ($p<0.01$; Fig. 3C)—a striking difference from
173 the lack of speed changes seen in *tax-2* mutants. Furthermore, *tax-4* mutants exhibited significantly increased

174 basal locomotion rates in both chambers (Fig 3B), suggesting that alterations in basal locomotion do not
175 interfere with experience-dependent movement adjustments.

176 Consistent with the idea that basal and experience-dependent locomotion are regulated independently,
177 we found that wild type worms cultivated at either 23ºC or 17ºC and then transferred to 20ºC during chamber
178 exploration exhibited significantly changes in basal locomotion speed but had little corresponding effect on the
179 extent of context-dependent modulation (Supp Fig. 2A). Specifically, temperature shifts were positively
180 correlated with basal locomotion rates (binary chambers: $r = 0.52$, $p < 0.0001$; uniform chambers: $r = 0.48$, $p <$
181 0.0001; Suppl. Fig. 2B), yet no significant correlation was observed between temperature shifts and ∆speed (r
182 $= -0.03$, $p = 0.22$; Suppl. Fig. 2C), reinforcing the idea that these two processes operate independently.

183 Together, these observations indicate that TAX-2 is critical for integrating prior experience into locomotion
184 modulation, while TAX-4 primarily regulates basal locomotion. Despite both pathways engaging cGMP
185 signaling, their functional independence suggests distinct regulatory mechanisms for basal locomotion and
186 context-dependent adjustments.

187 Given that four other genes (*cng-1, cng-2, cng-3* and *cng-4*) are predicted to encode CNG channels in *C.*
188 *elegans,* we investigated their role in locomotion modulation in microfluidic chambers [67]. Due to abnormal
189 development in *cng-1* mutants, we were unable to assess their locomotion; however, we were able to evaluate
190 mutants of the other three genes. We found that *cng-3(gk541751)* mutant worms failed to adjust locomotion
191 speed in the microfluidic chambers, while *cng-2(tm4267)* and *cng-4(gk195496)* mutants exhibited normal
192 modulation comparable to wild type worms (Fig. 3D). The identification of CNG-3 was particularly intriguing, as
193 recent studies suggest that it mediates changes in AFD neuronal activity based on prior temperature
194 experiences [68,69], indicating that CNG-3 contributes to neural plasticity rather than direct stimulus detection.
195 Our results further support this view by showing that CNG-3 plays a broader role in locomotion modulation in
196 environments lacking thermal gradients, which suggests its involvement in neuronal plasticity beyond the
197 thermosensory modality.

198 Next, we determined whether AFD is the site where CNG-3 functions in context-dependent locomotion
199 modulation. To do so, we introduced single-copy transgenes expressing *cng-3* cDNA under the control of two
200 AFD-specific promoters, *srtx-1Bp* and *gcy-18p*, into *cng-3(gk541751)* mutant worms. Regardless of the
201 promoter used, AFD-specific expression of *cng-3* restored the locomotion speed modulation (∆speed: 47 ± 8%

202 for *srtx-1Bp*::*cng-3* and 40 ± 6% for *gcy-18p::cng-3*) to levels similar to wild type (Fig 3E). These results
203 demonstrate that AFD neurons are the site of action for CNG-3 in mediating context-dependent locomotion
204 modulation. Overall, our findings elucidate an unexplored role for AFD beyond thermosensation, revealing that
205 components of a cGMP signaling pathway enable AFD to modulate behavior in an experience-dependent
206 manner.
207
208 **AFD sensory microvilli are dispensable for locomotion modulation, but AFD neurons are required.**
209 The finding that cGMP signaling genes (such as *gcy-18* and *cng-3*) in AFD neurons modulate context-
210 dependent locomotion prompted us to investigate whether the AFD thermosensory apparatus, crucial for
211 temperature detection [36], is also necessary for locomotion modulation in our microfluidic assay. Previous
212 studies have shown that the sensory microvilli at the tip of the AFD dendrite (Fig. 4A) are essential for
213 temperature sensing and thermotaxis [36,38]. For example, mutations in the *kcc-3* gene, which encodes a
214 K^+/Cl^- cotransporter in the amphid sheath glia, disrupt microvilli formation and significantly impair thermotaxis
215 towards their cultivation temperature [37]. Despite these thermotaxis defects, we found that context-dependent
216 locomotion modulation remained unchanged in *kcc-3(ok228)* mutant worms (Δspeed: 33 ± 4%) compared to
217 wild type (42 ± 7%; p = 0.28; Fig. 4B, C). Interestingly, *kcc-3* mutant worms displayed elevated basal
218 locomotion rates in both chamber types (Fig. 4B), a phenomenon also observed in *tax-4* mutants. This further
219 supports our earlier finding that alterations in basal locomotion do not correlate with context-dependent
220 locomotion modulation (Suppl. Fig. 2B, C). Together, these findings suggest that the role of AFD neurons in
221 modulating context-dependent locomotion is distinct from their thermosensory functions and differs from the
222 mechanisms controlling basal locomotion.
223 To further confirm that the sensory endings of AFD are not required for context-dependent locomotion
224 modulation, we examined *ttx-1(767)* mutant worms, which completely lack microvilli and exhibit more severe
225 thermotaxis defects than those seen in *kcc-3* mutants [38]. Consistent with the notion that AFD has separate
226 roles in context-dependent locomotion and thermosensation, *ttx-1* mutants still display locomotion modulation
227 in microfluidic chambers. However, the extent of modulation in these mutants was slightly reduced and more
228 variable (Δspeed: 29 ± 10%) compared to wild type animals (42 ± 7%, p = 0.29, Fig. 4D). It is worth noting that
229 *ttx-1* mutations disrupt the expression of multiple AFD genes, including those involved in cGMP signaling [70],

230 which may explain the increased variability in locomotion modulation. Nonetheless, despite completely lacking
231 the AFD sensory apparatus, the ability of *ttx-1* mutant worms to adjust their locomotion speed further
232 demonstrates that AFD neurons modulate context-dependent locomotion via mechanisms distinct from those
233 used in thermosensation.

234 Surprised to find that the AFD sensory apparatus is dispensable for locomotion modulation, we next
235 examined worms with genetically ablated AFD neurons. To achieve targeted AFD ablation, we used a
236 published strain with an integrated transgene expressing caspase protein under the AFD-specific promoter
237 *gcy-8p* [71]. AFD-ablated worms lost the ability to adjust locomotion rates in microfluidic chambers, as
238 indicated by a significant reduction in Δspeed (wild type: 42 ± 7%, AFD ablated: -2 ± 7%, $p < 0.001$; Fig. 4E).
239 These results demonstrate that although the sensory endings of AFD are not required for locomotion
240 adjustment, the AFD neuron itself is essential.

241

242 **Context-dependent locomotion modulation requires the MEC-10 mechanosensory channel subunit.**

243 We investigated whether mechanosensation is necessary for worms to perform context-dependent
244 locomotion adjustments in microfluidic chambers. This was prompted by previous findings showing that touch
245 sensation is critical for *C. elegans* to select their preferred space through interactions with physical structures
246 [52]. The *mec-10* gene encodes an amiloride-sensitive Na^+ channel protein required for sensing body touch.
247 Mutations in *mec-10* disrupt mechanotransduction channels in the worms touch-receptor neurons (TRNs),
248 impairing touch sensitivity [72,73]. We found that *mec-10(tm1552)* mutants failed to display locomotion
249 adjustment (Δspeed: 5 $\pm$ 4%, Fig. 5B). These results show that *mec-10* is crucial for context-dependent
250 locomotion modulation, supporting the hypothesis that locomotion is modulated depending on the worm's
251 tactile experience.

252

253 **AIB interneurons connecting TRNs and AFD are crucial for tactile-dependent behavioral plasticity.**

254 Touch receptor neurons (TRNs) do not directly synapse onto AFD, suggesting that additional neurons are
255 required to bridge them for tactile-dependent locomotion modulation. Examination of the *C. elegans*
256 connectome revealed that AIB serves as the shortest network pathway connecting TRNs to AFD (Fig. 5A). This
257 positions AIB as a key candidate for relaying signals from TRNs to AFD. If this is correct, we expect AIB to be

258 necessary for tactile-dependent modulation. To examine this, we quantified the locomotion of AIB-ablated
259 worms in microfluidic chambers. For this, we employed a previously published strain expressing caspase
260 under an AIB-specific promoter (*npr-9p*), resulting in ablation of the AIB neuron pair [74]. We found AIB-ablated
261 worms failed to adjust their speed in chambers, showing a significant reduction in ∆speed (-1 ± 5%) compared
262 to wild type (32 ± 8%, $p < 0.01$, Fig. 5C). These results demonstrate that the AIB interneurons are crucial for
263 tactile-dependent locomotion modulation.
264

265 **Mutations in *innexin* genes disrupt tactile-dependent modulation.**

266 Electrical synapses between AIB and AFD in *C. elegans* are formed by gap junction proteins called
267 innexins [75]. If these AIB–AFD connections are important for tactile-dependent modulation, then mutations in
268 innexin genes should impair locomotion adjustments in microfluidic chambers. To examine this hypothesis, we
269 investigated loss-of-function mutants of various innexin genes. Because *C. elegans* has 25 innexin genes
270 [76,77], we focused on those known to be expressed in AFD and AIB [78–80], identifying three genes (*inx-4,*
271 *inx-10* and *inx-19)* expressed in AFD*,* one gene (*inx-1)* in AIB, and one gene (*inx-7*) in both*.* We found that *inx-*
272 *10* mutants exhibited a partial but significant decrease in locomotion adjustments (∆speed: 15 ± 3%) compared
273 to wild type worms (45 ± 7%, $p < 0.001$, Fig. 6A). Similarly, mutations in *inx-1, inx-4, and inx-7* all lowered
274 ∆speed values, although these differences were not statistically significant relative to wild type worms (Fig.
275 6A). Furthermore, we found that *inx-7; inx-10* double mutants exhibit a lower ∆speed compared to *inx-7* or *inx-*
276 *10* single mutants (Fig. 6B). These findings suggest that disrupting innexins in AFD and AIB impair tactile-
277 dependent locomotion modulation.
278

279 **Re-establishing AIB-AFD electrical synapses restores tactile-dependent locomotion modulation in *inx-***
280 ***7; inx-10* double mutants.**

281 If the tactile-dependent modulation defects in innexin mutants result from disrupted AIB-AFD electrical
282 synapses, then reintroducing a synthetic gap junction specifically between these neurons should rescue
283 locomotion modulation. To test this, we employed a recently developed approach that introduces engineered
284 electrical synapses by expressing the mammalian gap junction protein Cx36 in *C. elegans* neurons. Several
285 studies have shown that engineered Cx36 synapses in *C. elegans* facilitate electrical coupling between

neurons, support behavioral modulation, and circumvent chemosensory impairments in damaged neural circuits [81–84]. Based on these findings, we introduced Cx36 into AFD and AIB neurons in *inx-7; inx-10* double mutants (Fig. 6C). Remarkably, expression of Cx36 in both AFD and AIB significantly improved locomotion adjustments in *inx-7; inx-10* mutants, increasing Δspeed from 15 ± 3% to 31 ± 8% ($p < 0.05$, Fig. 6D). These findings demonstrate that engineered electrical synapses between AFD and AIB can restore tactile-dependent locomotion modulation.

DISCUSSION

Our study reveals that the thermosensory AFD neuron plays an unexpected role in coupling tactile experiences to locomotion modulation in *C. elegans*. We show that: 1) *C. elegans* exhibit distinct locomotion patterns in identical environments, influenced by prior tactile experiences; 2) tactile-dependent behavior modulation requires the AFD neuron but not its thermosensory dendritic endings; 3) thermotaxis and tactile-dependent locomotion modulation rely on distinct sets of cGMP signaling proteins and CNG channel subunits; 4) the AIB interneuron, which connects AFD to mechanosensory circuits, is essential for tactile modulation; and 5) electrical synapses between AFD and AIB are critical for this process. Below, we discuss the implications of these findings.

A thermosensation-independent role for AFD in tactile-dependent behavior modulation.

Our findings highlight the remarkable versatility of sensory neurons in shaping behaviors beyond their primary functions. This supports the emerging view that sensory neurons have multifaceted roles in circuit modulation, extending well beyond canonical sensory activities. Such complexity is encoded at multiple levels within neural circuits. In *C. elegans*, for instance, the ASH neuron drives avoidance responses to various noxious stimuli, including hyperosmolarity, nose touch, and volatile repellents, demonstrating polymodal functionality [85–88]. Similarly, the olfactory receptor neuron AWC exhibits stochastic responses to temperature, introducing variability that enhances the flexibility and reliability of thermotactic behavior [89–91]. In contrast to these examples, the role of AFD in tactile-dependent plasticity does not rely on its sensory endings but is mediated through synaptic connectivity. This reveals an unexpected mechanism by which AFD

influences context-dependent behavioral plasticity via network-level interactions rather than direct sensory activity.

Distinct cGMP signaling pathways in AFD mediate sensation and plasticity.

Our data indicates that the CNG channel α subunits TAX-4 and CNG-3 play distinct roles in AFD function. Previous work has shown that TAX-4 is essential for AFD to detect temperature and generate thermally evoked responses [40], whereas CNG-3, although dispensable for temperature sensing, is crucial for tactile-dependent locomotion modulation. Supporting a broader role in sensory plasticity, CNG-3 is required in AWC neurons for short-term odor adaptation [92] and in AFD for adjusting temperature thresholds based on prior thermal experiences [68]. Our demonstration of the essential role of CNG-3 in tactile-dependent locomotion modulation further suggests that CNG-3 enables context-dependent behavioral plasticity rather than directly mediating stimulus detection.

CNG channels are heteromeric complexes composed of both α and β subunits. Our data, along with previous work, show that TAX-2, the CNG β subunit in *C. elegans*, is required for both tactile-dependent locomotion modulation and thermotransduction [40]. This finding implies that TAX-2 can partner with different α subunits to support sensory detection and neural plasticity. This functional specialization is reminiscent of photoreceptor neurons, where the composition and ratio of CNG channel subunits determine light sensitivity and enable contrast detection under varying light intensities [93–95].

In addition to the diversity of CNG channels, guanylyl cyclases in AFD also exhibit functional specificity. For example, mutations in *gcy-18* alone significantly disrupt tactile-dependent locomotion modulation without substantially affecting temperature sensing [41,43], whereas *gcy-8* is essential for generating thermally evoked Ca^{2+} responses [41,42] yet appears dispensable for tactile-dependent plasticity. Together, these results show that AFD uses distinct sets of guanylyl cyclases and CNG channels to execute dual roles—precise temperature sensing and context-dependent behavioral modulation.

Differential regulation of context-dependent plasticity and basal locomotion rates in AFD.

Our results further suggest that the mechanisms controlling basal locomotion and context-dependent behavioral modulation are not only distinct but also operate independently. Temperature fluctuations

significantly affect basal locomotion rates, i.e., higher temperatures accelerate speed, while lower temperatures slow it down [96,97]. However, tactile-dependent locomotion modulation in microfluidic chambers remains robust despite these temperature-induced changes in basal movement. This independence is further supported by our observations in *tax-4* and *kcc-3* mutants, which display elevated basal locomotion rates yet still adjust their locomotion in response to tactile experiences. These findings indicate that the processes governing basal locomotion and context-dependent modulation are controlled by separate, non-interfering mechanisms, even though both pathways engage cGMP signaling.

Electrical synapses bridge distinct circuits for behavioral modulation.

AIB-AFD electrical synapses are pivotal for tactile-dependent behavioral plasticity, serving to connect mechanosensory and thermosensory circuits. Our results show that disrupting the electrical connection between AFD and AIB impairs tactile-dependent locomotion modulation, whereas reintroducing engineered synapses restores it. The successful replacement of invertebrate innexins with vertebrate connexins, proteins that perform similar functions despite lacking sequence homology, indicates that the core function of these synapses lies in their connectivity rather than in their specific protein sequences. Previous models have proposed that AIB-AFD electrical synapses contribute to avoidance behavior by forming part of an FLP-AIB-AFD circuit, with AIB serving as a hub neuron that integrates sensory inputs via chemical synapse with FLP and electrical synapse with AFD [98]. Our experiments using engineered synapses elucidate the functional importance of the AIB-AFD connection in tactile-dependent locomotion modulation. Moreover, the transfer of signaling molecules such as Ca^{2+} and cGMP through electrical synapses likely facilitates the coordination of neuronal activity across distinct networks [99–102]. Although the precise mechanisms require further investigation, our study demonstrates that AIB-AFD electrical synapses are essential for incorporating tactile context into locomotion modulation.

IN SUMMARY, our findings reveal an unexpected role for AFD in tactile-dependent behavioral plasticity. They show that specialized molecular mechanisms (including distinct cGMP signaling pathways, diverse guanylyl cyclases, and functional electrical synapse connectivity) enable AFD sensory neurons to perform dual

369 functions: detect stimuli and support context-dependent plasticity. This work expands our understanding of
370 sensory neuron versatility supporting adaptive behavior in animals.
371
372 **ACKNOWLEDGEMENTS**. This research was supported by NIH grants R01NS109476 and R01NS115974 to
373 JB. MR was supported by T32GM136534 and F31NS129545. The authors thank the Caenorhabditis elegans
374 Genetics Center (funded by the NIH Office of Research Infrastructure Programs P40 OD010440) for providing
375 worm strains. We also thank Lin Zhang and Yan Liu for their support in constructing DNA plasmids and
376 generating transgenic worm strains. Special thanks to Melissa Woo (Mercer Island High School), Tabitha Ngo,
377 and Sahithi Challam (Interlake High School) for their assistance with worm maintenance. We appreciate the
378 members of the Bai lab for their critical reading of the manuscript. Additionally, we acknowledge the multiple
379 mentorship programs at Fred Hutchinson Cancer Center, including the SURP Undergraduate Researchers and
380 Pathways Undergraduate Researchers programs, supported in part by the Cancer Center Support Grant P30
381 CA015704, for fostering relationships with high school and undergraduate trainees who contributed to this
382 project.
383

384 METHODS

385

386 **Nematode Strains and Growth –** *C. elegans* strains were maintained under standard conditions at 20°C on
387 nematode growth medium (NGM) agar plates [103]. These plates were seeded with *E. coli* OP50 lawns.
388 Strains used in this study are listed in Table 1.
389

390 **Single Copy Insertion of Transgenes –** *Mos1*-mediated transgene insertion methods were used to generate
391 transgenic animals carrying single-copy transgenes [104,105]. Briefly, worms carrying the *ttTi5605 Mos1* site
392 on chromosome II were injected with a mixture of plasmids encoding the transgene of interest (40 ng/µl) and
393 Cas9 protein plus guide RNA specific to the *Mos1* site (60 ng/µl). To aid in selection of successful insertions,
394 the inserted transgene also included markers *vha-9p::mScarlet* and *rps-0p::hygR*, which confer red
395 fluorescence in the gut and hygromycin resistance, respectively.
396

Transgenes and Germline Transformation – Strains carrying extrachromosomal arrays were generated by microinjecting various plasmids together with co-injection markers. The co-injection markers included *unc-112p::gfp* (coelomocyte, 30 ng/µl), *rpl-28p::neoR* (20 ng/µl), and *Cbr-unc-119* (20 ng/µl). The blank vector pBluescript was used as filler DNA to bring the final total DNA concentration to 100 ng/µl. A detailed list of the plasmids used to create transgenic worms in this study is provided in Table 2.

Fabrication of PDMS Microfluidic Chambers – Microfluidic chambers were designed in AutoCAD (S1. File), and the resulting CAD designs were used to fabricate SU8-Silicon molds with a height of 100 µm using photolithography (FlowJem, NO, Canada). These molds were then used to fabricate microfluidic chambers with various physical features using soft lithography with polydimethyl siloxane (PDMS, Sylgard 184, Dow Corning, MI). Specifically, PDMS prepolymer was poured onto the SU8-silicon molds and cured at 80°C for 2 hours. Once cured, the PDMS layer was carefully lifted away from the silicon wafer, and a 2 mm skin biopsy punch (Acuderm Inc., FL) was used to create inlet and outlet holes. To assemble the device, the PDMS layer was place onto a microscope slide (1 mm thick), and the assembly was treated in a plasma cleaner (PDC-32G, Harrick Scientific, NY) for 1 minute. Distilled water was added to the plasma-treated devices within 5 minutes. Before loading the worms, the devices were thoroughly rinsed with M9 buffer.

Behavior Analysis – Worms were age-synchronized for behavioral assays by transferring 40–50 young adult worms onto an NGM plate seeded with OP50 and allowing them to lay eggs for 2 hours before removal. The plates were then kept at room temperature (20 ± 2°C) for 72 hours, allowing the eggs to develop into young adults. To wash the synchronized adults off the plate, worms were gently transferred into Eppendorf tubes using glass Pasteur pipettes. After allowing the worms to settle at the bottom of the tube (~1 minute), the supernatant was removed and replaced with fresh M9 buffer. This washing step was repeated three times to remove residual OP50. Next, approximately 30–70 worms were loaded into the chamber inlet using a 20µl pipette and allowed to explore the chamber freely for 60 minutes before recording. Videos were captured for 10 seconds at 7.5 frames per second using a Basler acA2440 camera (Basler, PA) equipped with an AF Micro-NIKKOR 60 mm lens (Nikon, NY). Behavioral data were extracted from the videos using WormLab software (MBF Bioscience, VT) through individual worm tracking. Only those worms that were already within the assay

area at the start of the recording were analyzed, and any worms that entered later were excluded. Crawling speed was determined by the total distance traveled by a worm during the 10 second recording. A turn was defined as a change in crawling direction of 15° or more. Reversals were defined as sudden movement in the opposite direction for at least 5 frames (~0.6 seconds). Worms were considered idle if their absolute velocity (distance traveled between frames) was below 20 μm/s for more than 10 frames (~1.3 seconds).

Statistical Analysis – Behavior measurements were calculated for each individual chamber, and these chamber-specific values were then used to generate the final mean values shown in the bar plots. The sample size was defined as the number (approximately 25) of chambers analyzed per experiment. An unpaired Student's t-test with Bonferroni correction was used to compare average speeds between uniform and binary chambers. To quantify the relative difference between groups, we calculated the percent change for each value in the uniform chambers relative to the mean of value from the binary chambers. Specifically, we subtracted the mean of the values from the binary chamber from each individual value in the uniform chamber. The result was then divided by the mean of the binary chamber and multiplied by 100 to express the difference as a percentage. For comparisons among multiple strains, we conducted one-way ANOVA followed by a Tukey–Kramer post hoc test on all possible pairwise comparisons. All statistical analyses were performed using R.

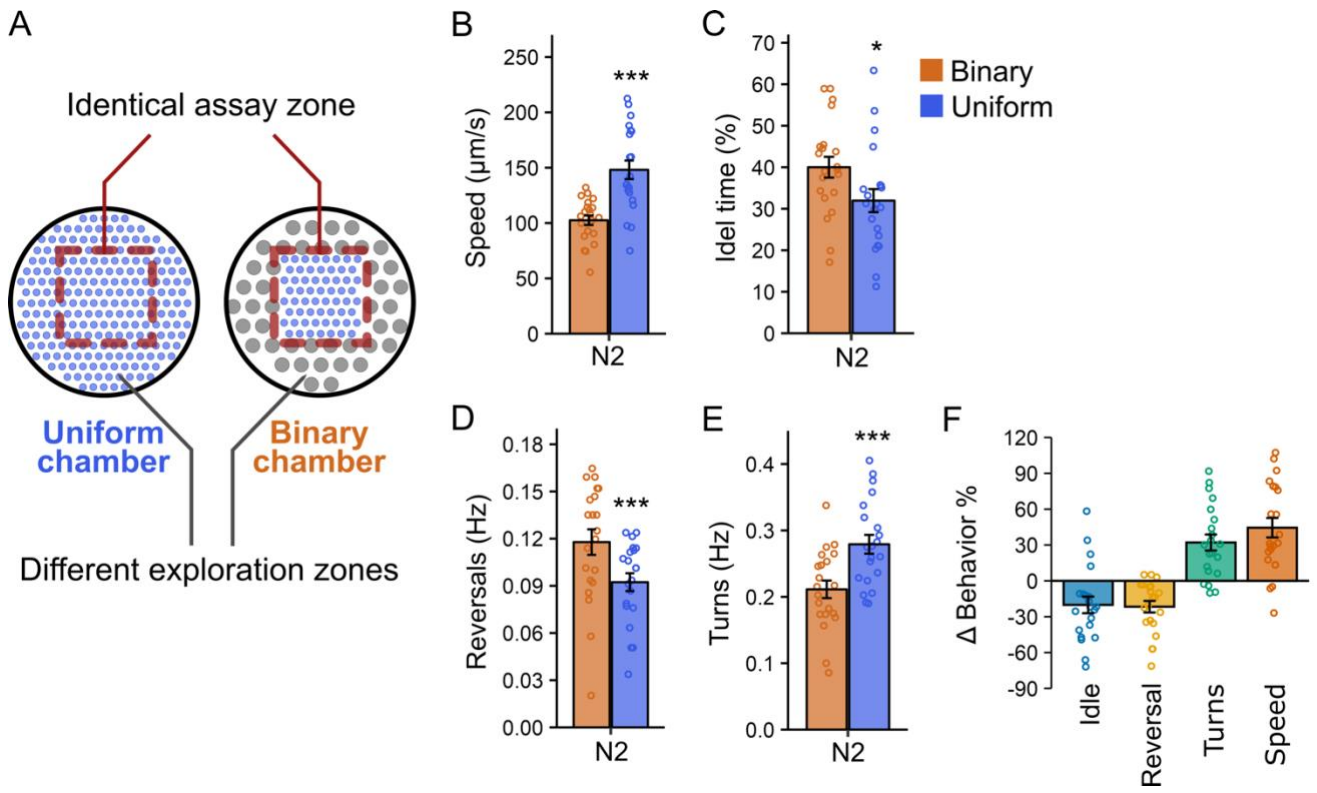

Figure 1. *C. elegans* displays distinct locomotion in identical environments after exploring different surrounding areas. (A) Schematic of two microfluidic chamber designs—uniform and binary—used for behavioral assays. Both chambers feature an identical assay area (red dashed-line boxes) where locomotion was analyzed, while the exploration zones contain distinct PDMS pillar patterns for worm exploration. (B–E) Bar graphs showing locomotion properties of wild type N2 worms in the assay zones of both chamber types after 1 hour of exploration. Data from binary chambers are shown in orange and from uniform chambers in blue. Shown are (B) locomotion speed, (C) percentage of time spent idle, (D) reversal frequency, and (E) turning frequency. Error bars represent standard error of the mean (SEM); each data point represents the mean behavior value of worms within a chamber. (F) Percent changes in locomotion properties, calculated from data in panels B–E and normalized to the mean value obtained from binary chambers (see Methods), are presented as mean ± SEM. Statistical significance was determined using an unpaired Student's t-test (***: $p < 0.001$, *: $p < 0.05$).

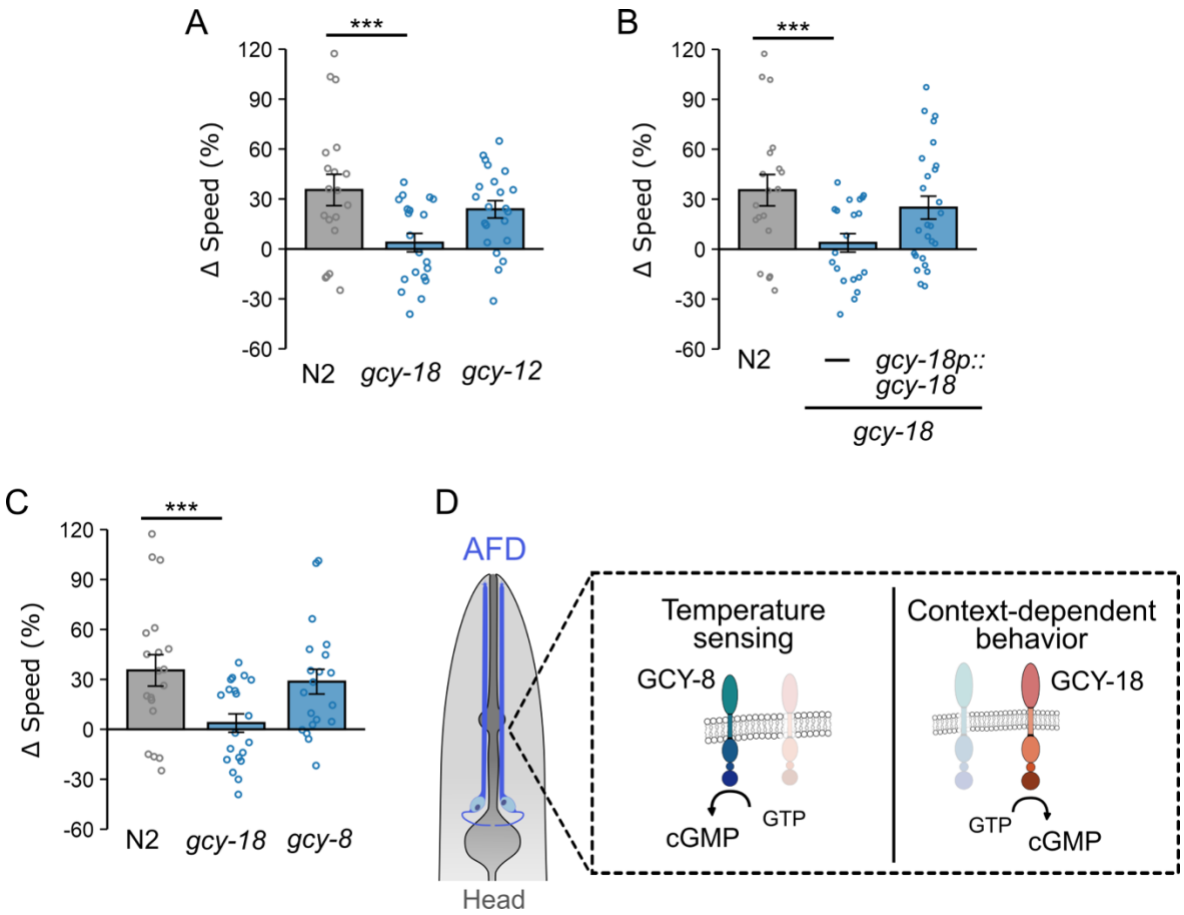

Figure 2. Guanylate cyclase gene *gcy-18* functions in AFD to mediate context-dependent locomotion modulation. (A) Speed differences (Δspeed) between uniform and binary chambers of wild type N2, *gcy-18* and *gcy-12* mutant worms. ΔSpeed was calculated as the percent change in locomotion rates in uniform chambers, relative to the mean of values obtained in binary chambers (see Methods). Mutant worms lacking *gcy-18* failed to demonstrate context-dependent adjustments in locomotion speed, as indicated by a low Δspeed value, whereas *gcy-12* mutants behaved similarly to wild type worms. (B) A single-copy transgene expressing *gcy-18* cDNA under the control of the *gcy-8* promoter in AFD restores context-dependent locomotion modulation. (C) Disruption of *gcy-8* does not impair context-dependent locomotion modulation. (D) Schematic illustrating the distinct roles of guanylate cyclase genes in AFD sensory neurons: *gcy-8* is required for thermosensation but not for context-dependent locomotion modulation, whereas *gcy-18* is essential for context-dependent locomotion modulation and plays only a moderate role in thermosensation. Data are presented as mean ± SEM. Each data point represents the mean behavior of worms within a single chamber. Statistical significance was determined using one-way ANOVA followed by a Tukey–Kramer post hoc test (***: $p < 0.001$).

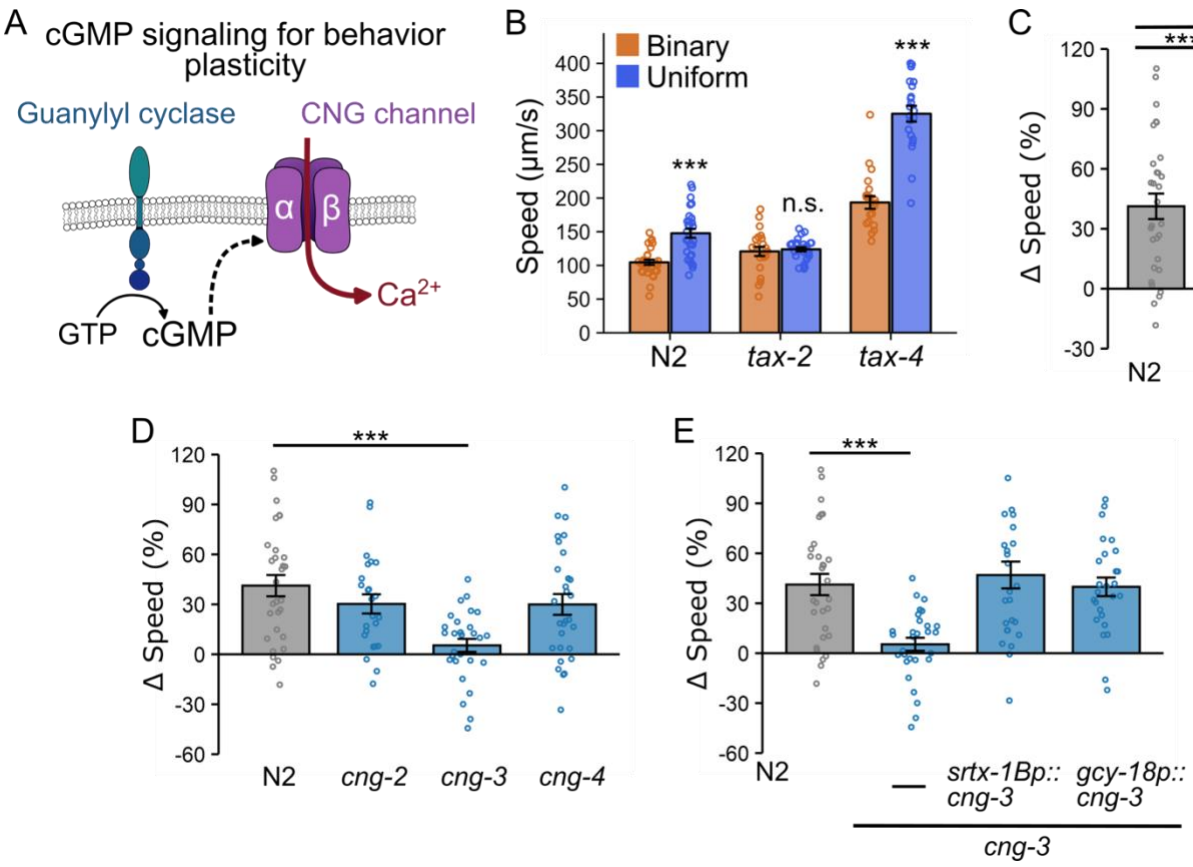

Figure 3. Cyclic nucleotide-gated (CNG) channel subunits TAX-2 and CNG-3 are required for locomotion modulation, but TAX-4 is not. (A) Schematic representation of CNG channel function. CNG channels are activated by cyclic nucleotides (such as cGMP) and mediate Ca^{2+} influx, thereby influencing neuronal activity and animal behavior. (B) Locomotion speed (µm/s) of N2, *tax-2*, and *tax-4* mutant worms in binary (orange) and uniform (blue) chambers. The *tax-2* mutants exhibit identical locomotion rates in both chamber types, whereas worms lacking *tax-4* display accelerated basal locomotion while still preserving context-dependent locomotion modulation. (C) Speed differences (Δspeed) for N2, *tax-2* mutant, and *tax-4* mutant worms. The *tax-2* mutants failed to modulate locomotion rates in a context-dependent manner, whereas *tax-4* mutations enhanced modulation. (D) Assessment of *cng-2*, *cng-3*, and *cng-4* roles in locomotion adjustments. The *cng-3* mutation abolishes locomotion modulation. (E) Single-copy transgenes expressing *cng-3* cDNA under two different AFD-specific promoters restore context-dependent locomotion adjustments. Data are presented as mean ± SEM. Each data point represents the mean behavior of worms within a single chamber. Statistical significance was determined using an unpaired Student's t-test to compare speeds between uniform and binary chambers (panel B) and one-way ANOVA followed by a Tukey–Kramer post hoc test to compare Δspeed across strains (panels C-E) (*: $p < 0.05$; **: $p < 0.01$, and ***: $p < 0.001$).

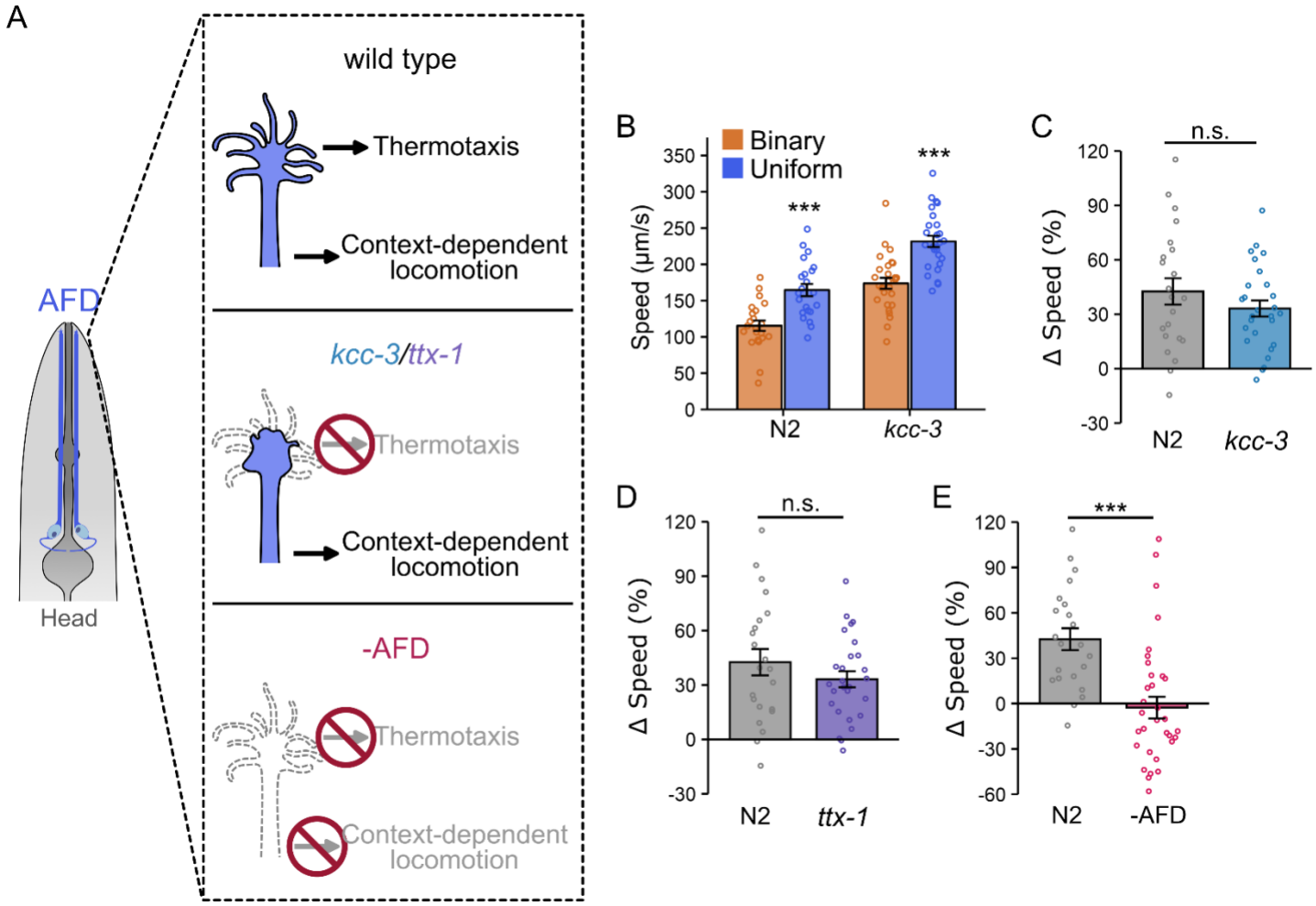

Figure 4. AFD, but not its sensory endings, is required for context-dependent locomotion modulation. (A) Schematic representation of AFD function in temperature sensing and locomotion modulation. AFD sensory endings are essential for thermosensation but dispensable for context-dependent locomotion modulation. (B) Locomotion speed (μm/s) of wild type N2 and *kcc-3* mutant worms in the binary (orange) and uniform (blue) chambers. The *kcc-3* mutants preserve context-dependent locomotion modulation while exhibiting increased basal locomotion rates. (C) Speed differences (Δspeed) for N2 and *kcc-3* mutant worms, and (D) for N2 and *ttx-1* mutant worms, respectively. Context-dependent locomotion modulation remains in *kcc-3* and *ttx-1* mutant worms, although they abolish the AFD thermosensory function. (E) Ablation of AFD eliminates the context-dependent locomotion modulation. Data are presented as mean ± SEM. Each data point represents the mean behavior of worms within a single chamber. Statistical significance was determined using an unpaired Student's t-text (n.s. indicates not significant, and ***: $p < 0.001$).

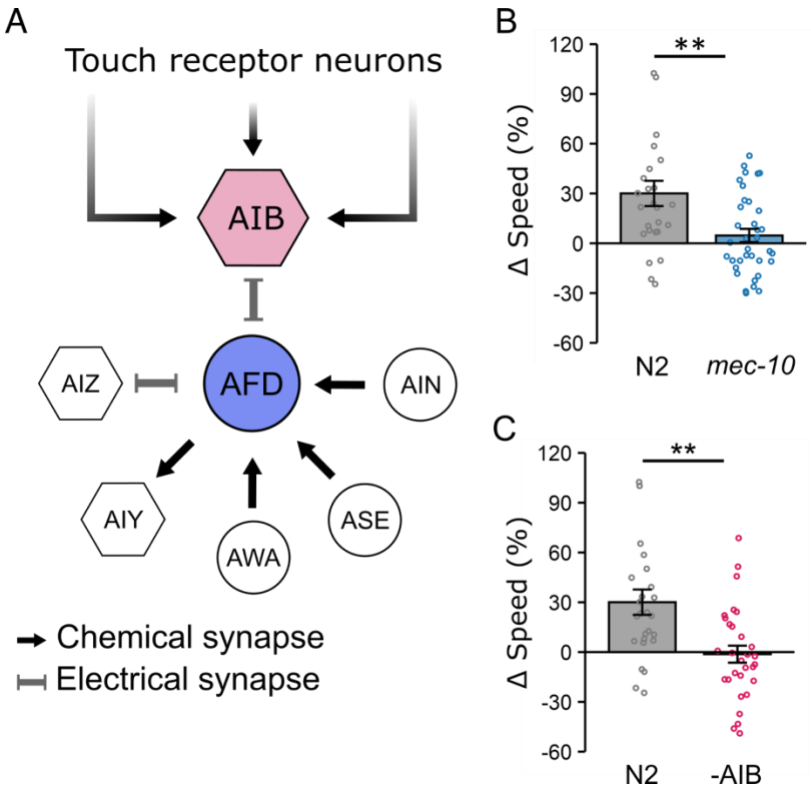

Figure 5. Context-dependent locomotion adjustments require both the mechanosensory channel subunit MEC-10 and the AIB interneurons that connect AFD to touch circuits. (A) Schematic representation of neurons synapsing with AFD. AIB provides the shortest pathway linking AFD to touch receptor neurons. (B, C) Speed differences (Δspeed) for N2, *mec-10* mutants, and AIB-ablated (-AIB) worms. Both *mec-10* mutants (B) and AIB-ablated worms (C) fail to modulate locomotion in microfluidic chambers. Data are presented as mean ± SEM. Each data point represents the mean behavior of worms within a single chamber. Statistical significance was determined using one-way ANOVA followed by a Tukey–Kramer post hoc test (**: $p < 0.01$).

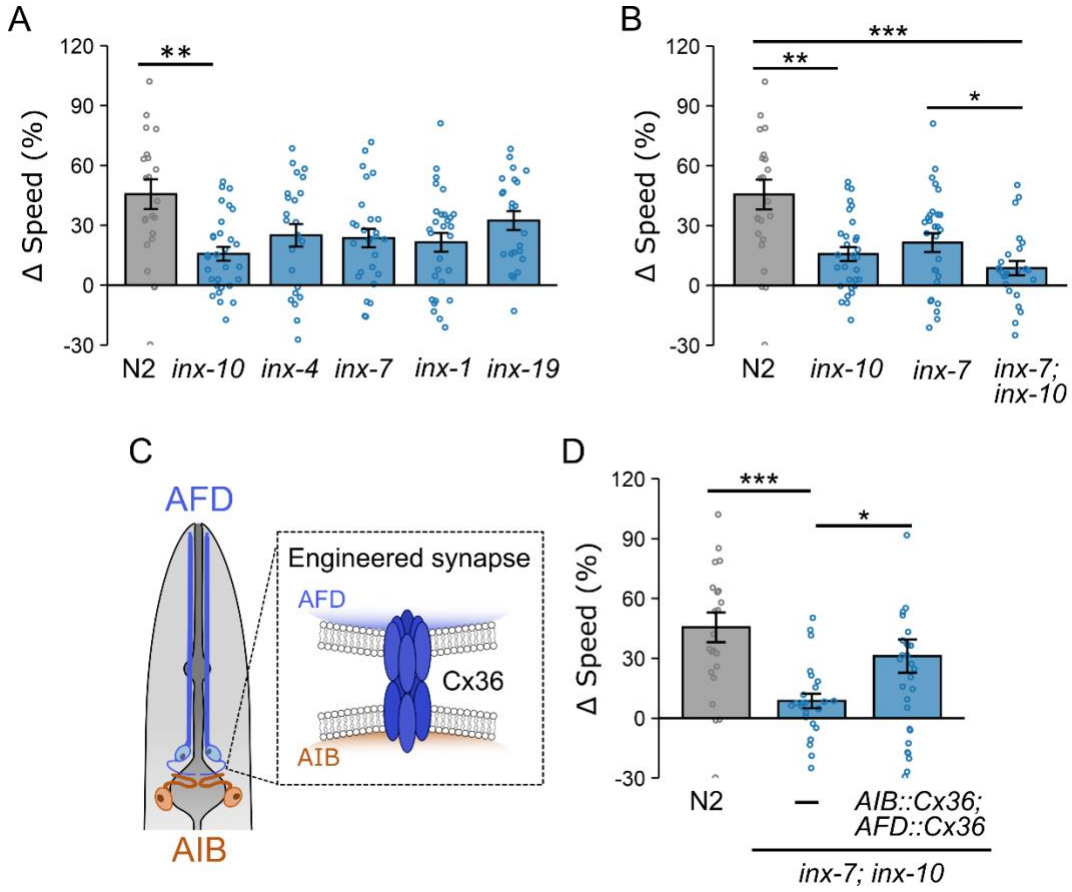

Figure 6. Tactile-dependent locomotion modulation is disrupted in mutant worms lacking gap junction genes and is restored by engineered Cx36 electrical synapses linking AFD and AIB. (A) Speed differences (Δspeed) for *inx-1, 4, 7, 10, 19* mutant worms. (B) Speed differences for *inx-7; inx-10* double mutants. (C) Schematic illustrating engineered electrical synapses formed by Cx36 when expressed in adjacent neurons. (D) Tactile-dependent locomotion modulation is restored in *inx-7; inx-10* double mutants by expressing Cx36 in AFD and AIB neurons. Data are presented as mean ± SEM. Each data point represents the mean behavior of worms within a single chamber. Statistical significance was determined using one-way ANOVA followed by a Tukey–Kramer post hoc test (*: $p < 0.05$; **: $p < 0.01$, and ***: $p < 0.001$).

515

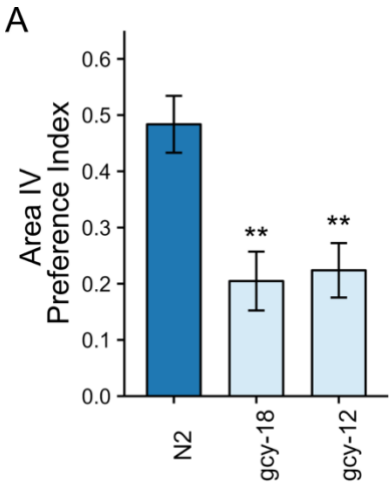

516

517 **Suppl. Figure 1.** Worms lacking either *gcy-18* or *gcy-12* failed to identify their preferred area in microfluidic
518 chambers. Preference index values of wild type N2 worms, *gcy-18* mutants, and *gcy-12* mutants were
519 determined as described by Han *et al.* [52]. Wild type worms exhibit a strong preference for a specific zone
520 (zone IV, as defined by Han *et al*. [52]), whereas both *gcy-18* and *gcy-12* mutants show significantly reduced
521 preference compared to wild type worms. Bars represent mean ± SEM. Statistical comparisons were
522 performed using one-way ANOVA followed by a Dunnett's test for multiple comparisons (**$p < 0.01$).

523

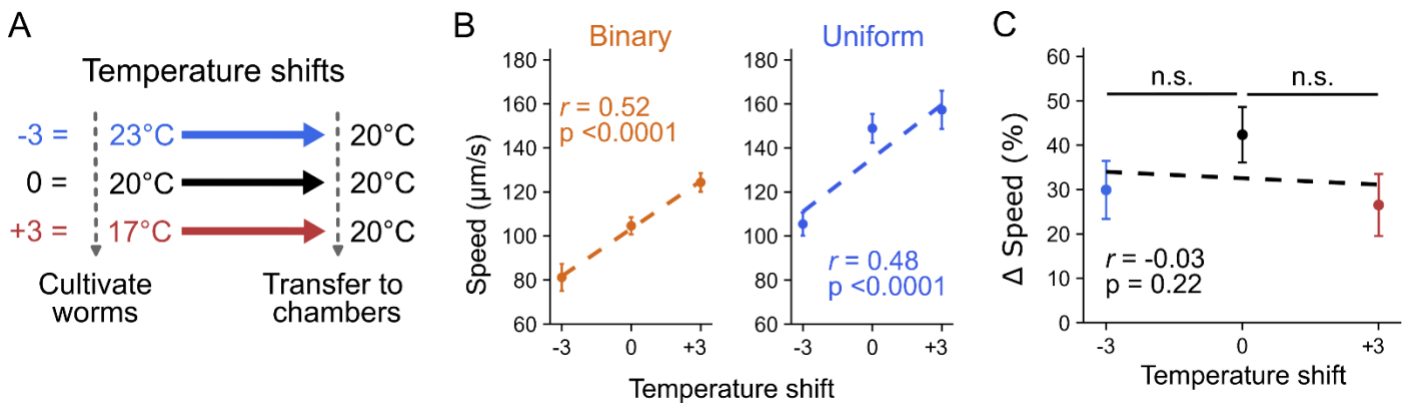

Suppl. figure 2. Temperature shifts do not affect tactile-dependent modulation. (A) Schematic of experimental design: Worms were reared at three different temperatures (17°C, 20°C, and 23°C) and then transferred to 20°C for 1 hour during the behavioral assay. (B) Locomotion speed of wild type N2 worms in the binary (orange) and uniform (blue) chambers after experiencing temperature shifts. Linear regression analysis reveals a significant positive correlation between rearing temperature and locomotion speed in both chambers. (C) Differences in speed (Δspeed) between worms experiencing different temperature shifts. Linear regression significance test shows no significant relationship between Δspeed and temperature shift. Points represent mean ± SEM.

547 **Table 1. List of *C. elegans* strains used in this study**

Strain	Genotype	Citation
PR694	*tax-2(p694) I*	[106]
PR678	*tax-4(p678) III*	[65]
FX31482	*cng-2(tm4267) IV*	[107]
VC40261	*cng-3(gk541751) IV*	[108]
VC20290	*cng-4(gk195496) IV*	[108]
IK800	*gcy-8(oy44) IV.*	[43]
VC30137	*gcy-18(gk423024) IV*	[108]
VC20451	*gcy-12(gk142661) II*	[108]
BJH3481	*gcy-18(gk423024) IV, pekSi609[gcy-18p::gcy-18(cDNA)::sl2::mNeonGreen::unc-54 3'utr, vha-6p::mScarlet, hygR(+)] ttTi5605 II*	This study
BJH3527	*pekSi655[srtx-1Bp::cng-3(cDNA)::sl2::mNeonGreen::unc-54 3'utr, vha-9p::mScarlet, hygR(+)] ttTi5605 II; cng-3(gk541751) IV*	This study
BJH3537	*tax-2(p694) I; pekSi665[srtx-1Bp::tax2(cDNA)::sl2::mNeonGreen ::unc-54 3'utr, vha-9p::mScarlet, hygR(+)] ttTi5605 II*	This study
BJH3539	*pekSi667 [gcy-18p::cng-3(cDNA)::sl2::mNeonGreen::unc-54* 3'utr, *vha-9p::mScarlet, hygR(+)] ttTi5605 II; cng-3(gk541751) IV*	This study
GN112	*pgIs2[gcy-8p::TU#813, gcy-8p::TU#814, unc-122p::GFP, gcy-8p::mCherry, gcy-8p::gfp, ttx-3p::gfp]*	[71]
LX1024	*kcc-3(ok228) II*	[37]
PR767	*ttx-1(p767) V*	[38]
JN578	*peIs578 [npr-9p::casp1 + npr-9p::venus + unc-122p::mCherry]* (genetically ablated AIB)	[74]
ZB2551	*mec-10(tm1552) X*	[72]
CB1611	*mec-4(e1611) X*	[109]
FG927	*inx-1(tm6662*) X.	[110]
FG0614	*inx-4 (ok2373) V*	[80]
RB1792	*inx-7(ok2319)* IV	[110]
RB2051	*inx-10(ok2714) V*	[110]
FX01896	*inx-19(tm1896) I*	[111]
BJH2919	*inx-7(ok2319) IV; inx-10(ok2714) V*	This study
BJH1162	*pekEx302 [srtx-1Bp::cx36*::sl2*::mNeonGreen, inx-1p::cx36* ::sl2*::mKate, Cbr-unc-119(+), unc-122p*::GFP, *neoR(+)]; unc-119(ed3) III; inx-7(ok2319) IV; inx-10(ok2714) V*	This study

548

549

550

551

552

553 **Table 2. List of plasmids used to create transgenic *C. elegans* strains**

Name	Contruct	Notes
BJP-MR16	*gcy-18p::gcy-18(mini-gene)::sl2::mNeonGreen::rab-3 3'utr; vha-9p::mScarlet::tbb-2 3'utr; rps-0p::hygR*	The *gcy-18* mini-gene includes all exons and introns 11, 12, and 13.
BJP-MR65	*srtx-1Bp::cng-3(cDNA)::sl2::mNeonGreen::rab-3 3'utr; vha-9p::mScarlet::tbb-2 3'utr; rps-0p::hygR*	
BJP-MR72	*srtx-1Bp::tax2(cDNA)::sl2::mNeonGreen::rab-3 3'utr; vha-9p::mScarlet::tbb-2 3'utr; rps-0p::hygR*	
BJP-MR93	*gcy-18p::cng-3(cDNA)::sl2::mNeonGreen::rab-3 3'utr; vha-9p::mScarlet::tbb-2 3'utr; rps-0p::hygR*	
BJP-MR96	*inx-1p::cx36::sl2::mKate::rab-3 3'utr*	
BJP-MR97	*srtx-1bp::cx36::sl2::mKate::rab-3 3'utr*	

554

555

556

557

558

559

560

561

562

563

564

565

566

567

568

569

REFERENCES

1. Navarro-Sánchez M, Gil-Miravet I, Montero-Caballero D, Castillo-Gómez E, Gundlach AL, Olucha-Bordonau FE. Some key parameters in contextual fear conditioning and extinction in adult rats. Behavioural Brain Research. 2024;462: 114874. doi:10.1016/j.bbr.2024.114874

2. Maren S, Phan KL, Liberzon I. The contextual brain: implications for fear conditioning, extinction and psychopathology. Nat Rev Neurosci. 2013;14: 417–428. doi:10.1038/nrn3492

3. Battaglia S, Garofalo S, di Pellegrino G. Context-dependent extinction of threat memories: influences of healthy aging. Scientific Reports. 2018;8: 12592. doi:10.1038/s41598-018-31000-9

4. Leitman DI, Wolf DH, Loughead J, Valdez JN, Kohler CG, Brensinger C, et al. Ventrolateral prefrontal cortex and the effects of task demand context on facial affect appraisal in schizophrenia. Soc Cogn Affect Neurosci. 2011;6: 66–73. doi:10.1093/scan/nsq018

5. Hadjikhani N, Joseph RM, Manoach DS, Naik P, Snyder J, Dominick K, et al. Body expressions of emotion do not trigger fear contagion in autism spectrum disorder. Social Cognitive and Affective Neuroscience. 2009;4: 70–78. doi:10.1093/scan/nsn038

6. Kipps CM, Nestor PJ, Acosta-Cabronero J, Arnold R, Hodges JR. Understanding social dysfunction in the behavioural variant of frontotemporal dementia: the role of emotion and sarcasm processing. Brain. 2009;132: 592–603. doi:10.1093/brain/awn314

7. Greimel E, Nehrkorn B, Fink GR, Kukolja J, Kohls G, Müller K, et al. Neural mechanisms of encoding social and non-social context information in autism spectrum disorder. Neuropsychologia. 2012;50: 3440–3449. doi:10.1016/j.neuropsychologia.2012.09.029

8. Badel L, Ohta K, Tsuchimoto Y, Kazama H. Decoding of Context-Dependent Olfactory Behavior in Drosophila. Neuron. 2016;91: 155–167. doi:10.1016/j.neuron.2016.05.022

9. Haberkern H, Basnak MA, Ahanonu B, Schauder D, Cohen JD, Bolstad M, et al. Visually Guided Behavior and Optogenetically Induced Learning in Head-Fixed Flies Exploring a Virtual Landscape. Current Biology. 2019;29: 1647-1659.e8. doi:10.1016/j.cub.2019.04.033

10. Sheintuch L, Geva N, Baumer H, Rechavi Y, Rubin A, Ziv Y. Multiple Maps of the Same Spatial Context Can Stably Coexist in the Mouse Hippocampus. Current Biology. 2020;30: 1467-1476.e6. doi:10.1016/j.cub.2020.02.018

11. Zars M, Zars T. High and low temperatures have unequal reinforcing properties in Drosophila spatial learning. J Comp Physiol A. 2006;192: 727–735. doi:10.1007/s00359-006-0109-6

12. Kishimoto Y, Kasamatsu S, Yanai S, Endo S, Akaike T, Ihara H. 8-Nitro-cGMP attenuates context-dependent fear memory in mice. Biochemical and Biophysical Research Communications. 2019;511: 141–147. doi:10.1016/j.bbrc.2019.01.138

13. Sasaki A, Sotnikova TD, Gainetdinov RR, Jarvis ED. Social Context-Dependent Singing-Regulated Dopamine. J Neurosci. 2006;26: 9010–9014. doi:10.1523/JNEUROSCI.1335-06.2006

14. Billeter J-C, Jagadeesh S, Stepek N, Azanchi R, Levine JD. Drosophila melanogaster females change mating behaviour and offspring production based on social context. Proceedings of the Royal Society B: Biological Sciences. 2012;279: 2417–2425. doi:10.1098/rspb.2011.2676

15. Wolfin MS, Raguso RA, Davidowitz G, Goyret J. Context dependency of in-flight responses by Manduca sexta moths to ambient differences in relative humidity. Journal of Experimental Biology. 2018;221. doi:10.1242/jeb.177774

16. Sawin ER, Ranganathan R, Horvitz HR. C. elegans Locomotory Rate Is Modulated by the Environment through a Dopaminergic Pathway and by Experience through a Serotonergic Pathway. Neuron. 2000;26: 619–631. doi:10.1016/S0896-6273(00)81199-X

17. Gourgou E, Adiga K, Goettemoeller A, Chen C, Hsu A-L. *Caenorhabditis elegans* learning in a structured maze is a multisensory behavior. iScience. 2021;24: 102284. doi:10.1016/j.isci.2021.102284

18. Dillon J, Holden-Dye L, O'Connor V, Hopper NA. Context-dependent regulation of feeding behaviour by the insulin receptor, DAF-2, in Caenorhabditis elegans. Invert Neurosci. 2016;16: 4. doi:10.1007/s10158-016-0187-2

19. Law E, Nuttley WM, Kooy D van der. Contextual Taste Cues Modulate Olfactory Learning in C. elegans by an Occasion-Setting Mechanism. Current Biology. 2004;14: 1303–1308. doi:10.1016/j.cub.2004.06.066

20. Kindt KS, Quast KB, Giles AC, De S, Hendrey D, Nicastro I, et al. Dopamine Mediates Context-Dependent Modulation of Sensory Plasticity in C. elegans. Neuron. 2007;55: 662–676. doi:10.1016/j.neuron.2007.07.023

21. Goetting DL, Soto R, Van Buskirk C. Food-Dependent Plasticity in Caenorhabditis elegans Stress-Induced Sleep Is Mediated by TOR-FOXA and TGF-β Signaling. Genetics. 2018;209: 1183–1195. doi:10.1534/genetics.118.301204

22. Susoy V, Hung W, Witvliet D, Whitener JE, Wu M, Park CF, et al. Natural sensory context drives diverse brain-wide activity during C. elegans mating. Cell. 2021; S0092867421009983. doi:10.1016/j.cell.2021.08.024

23. Ghosh DD, Sanders T, Hong S, McCurdy LY, Chase DL, Cohen N, et al. Neural Architecture of Hunger-Dependent Multisensory Decision Making in *C. elegans*. Neuron. 2016;92: 1049–1062. doi:10.1016/j.neuron.2016.10.030

24. Zhen M, Samuel AD. C. elegans locomotion: small circuits, complex functions. Current Opinion in Neurobiology. 2015;33: 117–126. doi:10.1016/j.conb.2015.03.009

25. Emmons SW. Neural Circuits of Sexual Behavior in Caenorhabditis elegans. Annual Review of Neuroscience. 2018;41: 349–369. doi:10.1146/annurev-neuro-070815-014056

26. Meisel JD, Kim DH. Behavioral avoidance of pathogenic bacteria by Caenorhabditis elegans. Trends in Immunology. 2014;35: 465–470. doi:10.1016/j.it.2014.08.008

27. Metaxakis A, Petratou D, Tavernarakis N. Multimodal sensory processing in Caenorhabditis elegans. Open Biol. 2018;8. doi:10.1098/rsob.180049

28. Stout Jr. RF, Verkhratsky A, Parpura V. Caenorhabditis elegans glia modulate neuronal activity and behavior. Front Cell Neurosci. 2014;8. doi:10.3389/fncel.2014.00067

29. Ward S, Thomson N, White JG, Brenner S. Electron microscopical reconstruction of the anterior sensory anatomy of the nematode caenorhabditis elegans. Journal of Comparative Neurology. 1975;160: 313–337. doi:10.1002/cne.901600305

30. Ware RW, Clark D, Crossland K, Russell RL. The nerve ring of the nematode Caenorhabditis elegans: Sensory input and motor output. Journal of Comparative Neurology. 1975;162: 71–110. doi:10.1002/cne.901620106

31. Ghosh DD, Nitabach MN, Zhang Y, Harris G. Multisensory integration in C. elegans. Current Opinion in Neurobiology. 2017;43: 110–118. doi:10.1016/j.conb.2017.01.005

32. Hobert O. Behavioral plasticity in C. elegans: Paradigms, circuits, genes. Journal of Neurobiology. 2003;54: 203–223. doi:10.1002/neu.10168

33. Komuniecki R, Hapiak V, Harris G, Bamber B. Context-dependent modulation reconfigures interactive sensory-mediated microcircuits in Caenorhabditis elegans. Current Opinion in Neurobiology. 2014;29: 17–24. doi:10.1016/j.conb.2014.04.006

34. Goodman MB, Sengupta P. The extraordinary AFD thermosensor of C. elegans. Pflugers Arch - Eur J Physiol. 2018;470: 839–849. doi:10.1007/s00424-017-2089-5

35. Clark DA, Biron D, Sengupta P, Samuel ADT. The AFD Sensory Neurons Encode Multiple Functions Underlying Thermotactic Behavior in Caenorhabditis elegans. J Neurosci. 2006;26: 7444–7451. doi:10.1523/JNEUROSCI.1137-06.2006

36. Yoshida A, Nakano S, Suzuki T, Ihara K, Higashiyama T, Mori I. A glial K+/Cl− cotransporter modifies temperature-evoked dynamics in Caenorhabditis elegans sensory neurons. Genes, Brain and Behavior. 2016;15: 429–440. doi:10.1111/gbb.12260

37. Singhvi A, Liu B, Friedman CJ, Fong J, Lu Y, Huang X-Y, et al. A Glial K/Cl Transporter Controls Neuronal Receptive Ending Shape by Chloride Inhibition of an rGC. Cell. 2016;165: 936–948. doi:10.1016/j.cell.2016.03.026

38. Satterlee JS, Sasakura H, Kuhara A, Berkeley M, Mori I, Sengupta P. Specification of Thermosensory Neuron Fate in C. elegans Requires ttx-1, a Homolog of otd/Otx. Neuron. 2001;31: 943–956. doi:10.1016/S0896-6273(01)00431-7

39. Aok I, Shiota M, Tsukada Y, Nakano S, Mori I. cGMP dynamics that underlies thermosensation in temperature-sensing neuron regulates thermotaxis behavior in C. elegans. PLOS ONE. 2022;17: e0278343. doi:10.1371/journal.pone.0278343

40. Ramot D, MacInnis BL, Goodman MB. Bidirectional temperature-sensing by a single thermosensory neuron in C. elegans. Nat Neurosci. 2008;11: 908–915. doi:10.1038/nn.2157

41. Wang D, O'Halloran D, Goodman MB. GCY-8, PDE-2, and NCS-1 are critical elements of the cGMP-dependent thermotransduction cascade in the AFD neurons responsible for C. elegans thermotaxis. J Gen Physiol. 2013;142: 437–449. doi:10.1085/jgp.201310959

42. Takeishi A, Yu YV, Hapiak VM, Bell HW, O'Leary T, Sengupta P. Receptor-type Guanylyl Cyclases Confer Thermosensory Responses in C. elegans. Neuron. 2016;90: 235–244. doi:10.1016/j.neuron.2016.03.002

43. Inada H, Ito H, Satterlee J, Sengupta P, Matsumoto K, Mori I. Identification of Guanylyl Cyclases That Function in Thermosensory Neurons of Caenorhabditis elegans. Genetics. 2006;172: 2239–2252. doi:10.1534/genetics.105.050013

44. Hedgecock EM, Russell RL. Normal and mutant thermotaxis in the nematode Caenorhabditis elegans. Proc Natl Acad Sci USA. 1975;72: 4061–4065. doi:10.1073/pnas.72.10.4061

45. Ryu WS, Samuel ADT. Thermotaxis in *Caenorhabditis elegans* Analyzed by Measuring Responses to Defined Thermal Stimuli. J Neurosci. 2002;22: 5727–5733. doi:10.1523/JNEUROSCI.22-13-05727.2002

46. Kuhara A, Ohnishi N, Shimowada T, Mori I. Neural coding in a single sensory neuron controlling opposite seeking behaviours in Caenorhabditis elegans. Nat Commun. 2011;2: 355. doi:10.1038/ncomms1352

688 47. Mori I, Ohshima Y. Neural regulation of thermotaxis in Caenorhabditis elegans. Nature. 1995;376: 344–348.
689 doi:10.1038/376344a0

690 48. Kuhara A, Mori I. Molecular Physiology of the Neural Circuit for Calcineurin-Dependent Associative Learning
691 in *Caenorhabditis elegans*. J Neurosci. 2006;26: 9355–9364. doi:10.1523/JNEUROSCI.0517-06.2006

692 49. Hobert O, D'Alberti T, Liu Y, Ruvkun G. Control of Neural Development and Function in a Thermoregulatory
693 Network by the LIM Homeobox Gene lin-11. J Neurosci. 1998;18: 2084–2096. doi:10.1523/JNEUROSCI.18-
694 06-02084.1998

695 50. Chung SH, Clark DA, Gabel CV, Mazur E, Samuel AD. The role of the AFD neuron in C. elegans thermotaxis
696 analyzed using femtosecond laser ablation. BMC Neurosci. 2006;7: 30. doi:10.1186/1471-2202-7-30

697 51. Ikeda M, Nakano S, Giles AC, Xu L, Costa WS, Gottschalk A, et al. Context-dependent operation of neural
698 circuits underlies a navigation behavior in Caenorhabditis elegans. PNAS. 2020;117: 6178–6188.
699 doi:10.1073/pnas.1918528117

700 52. Han B, Dong Y, Zhang L, Liu Y, Rabinowitch I, Bai J. Dopamine signaling tunes spatial pattern selectivity in C.
701 elegans. eLife. 2017;6. doi:10.7554/eLife.22896

702 53. Komatsu H, Jin Y-H, L'Etoile N, Mori I, Bargmann CI, Akaike N, et al. Functional reconstitution of a
703 heteromeric cyclic nucleotide-gated channel of Caenorhabditis elegans in cultured cells. Brain Research.
704 1999;821: 160–168. doi:10.1016/S0006-8993(99)01111-7

705 54. Finn JT, Krautwurst D, Schroeder JE, Chen T-Y, Reed RR, Yau K-W. Functional Co-assembly among Subunits
706 of Cyclic-Nucleotide-Activated, Nonselective Cation Channels, and Across Species from Nematode to
707 Human. Biophysical Journal. 1998;74: 1333–1345. doi:10.1016/S0006-3495(98)77846-4

708 55. Kaupp UB, Seifert R. Cyclic Nucleotide-Gated Ion Channels. Physiological Reviews. 2002;82: 769–824.
709 doi:10.1152/physrev.00008.2002

710 56. Xue J, Han Y, Zeng W, Jiang Y. Structural mechanisms of assembly, permeation, gating, and pharmacology of
711 native human rod CNG channel. Neuron. 2022;110: 86-95.e5. doi:10.1016/j.neuron.2021.10.006

712 57. Harris G, Shen Y, Ha H, Donato A, Wallis S, Zhang X, et al. Dissecting the Signaling Mechanisms Underlying
713 Recognition and Preference of Food Odors. J Neurosci. 2014;34: 9389–9403. doi:10.1523/JNEUROSCI.0012-
714 14.2014

715 58. He C, Altshuler-Keylin S, Daniel D, L'Etoile -->Noelle D., O'Halloran D. The cyclic nucleotide gated channel
716 subunit CNG-1 instructs behavioral outputs in Caenorhabditis elegans by coincidence detection of
717 nutritional status and olfactory input. Neuroscience Letters. 2016;632: 71–78.
718 doi:10.1016/j.neulet.2016.08.037

719 59. Herrero A, Yoshii T, Ispizua JI, Colque C, Veenstra JA, Muraro NI, et al. Coupling Neuropeptide Levels to
720 Structural Plasticity in Drosophila Clock Neurons. Current Biology. 2020;30: 3154-3166.e4.
721 doi:10.1016/j.cub.2020.06.009

722 60. Feketa VV, Nikolaev YA, Merriman DK, Bagriantsev SN, Gracheva EO. CNGA3 acts as a cold sensor in
723 hypothalamic neurons. Lishko PV, Aldrich RW, Tominaga M, Sobolevsky A, editors. eLife. 2020;9: e55370.
724 doi:10.7554/eLife.55370

725 61. Dolzer J, Schröder K, Stengl M. Cyclic nucleotide-dependent ionic currents in olfactory receptor neurons of
726 the hawkmoth Manduca sexta suggest pull–push sensitivity modulation. European Journal of Neuroscience.
727 2021;54: 4804–4826. doi:10.1111/ejn.15346

62. Kelliher KR, Ziesmann J, Munger SD, Reed RR, Zufall F. Importance of the CNGA4 channel gene for odor discrimination and adaptation in behaving mice. Proceedings of the National Academy of Sciences. 2003;100: 4299–4304. doi:10.1073/pnas.0736071100

63. Michalakis S, Kleppisch T, Polta SA, Wotjak CT, Koch S, Rammes G, et al. Altered synaptic plasticity and behavioral abnormalities in CNGA3-deficient mice. Genes, Brain and Behavior. 2011;10: 137–148. doi:10.1111/j.1601-183X.2010.00646.x

64. Haverkamp S, Michalakis S, Claes E, Seeliger MW, Humphries P, Biel M, et al. Synaptic Plasticity in CNGA3−/− Mice: Cone Bipolar Cells React on the Missing Cone Input and Form Ectopic Synapses with Rods. J Neurosci. 2006;26: 5248–5255. doi:10.1523/JNEUROSCI.4483-05.2006

65. Komatsu H, Mori I, Rhee J-S, Akaike N, Ohshima Y. Mutations in a Cyclic Nucleotide–Gated Channel Lead to Abnormal Thermosensation and Chemosensation in C. elegans. Neuron. 1996;17: 707–718. doi:10.1016/S0896-6273(00)80202-0

66. Kimura KD, Miyawaki A, Matsumoto K, Mori I. The *C. elegans* Thermosensory Neuron AFD Responds to Warming. Current Biology. 2004;14: 1291–1295. doi:10.1016/j.cub.2004.06.060

67. Wojtyniak M, Brear AG, O'Halloran DM, Sengupta P. Cell- and subunit-specific mechanisms of CNG channel ciliary trafficking and localization in C. elegans. J Cell Sci. 2013;126: 4381–4395. doi:10.1242/jcs.127274

68. Hill TJ, Sengupta P. Feedforward and feedback mechanisms cooperatively regulate rapid experience-dependent response adaptation in a single thermosensory neuron type. bioRxiv; 2023. p. 2023.12.05.570166. doi:10.1101/2023.12.05.570166

69. Cho S-W, Choi KY, Park C-S. A new putative cyclic nucleotide-gated channel gene, cng-3, is critical for thermotolerance in Caenorhabditis elegans. Biochemical and Biophysical Research Communications. 2004;325: 525–531. doi:10.1016/j.bbrc.2004.10.060

70. Kagoshima H, Kohara Y. Co-expression of the transcription factors CEH-14 and TTX-1 regulates AFD neuron-specific genes gcy-8 and gcy-18 in C. elegans. Developmental Biology. 2015;399: 325–336. doi:10.1016/j.ydbio.2015.01.010

71. Glauser DA, Chen WC, Agin R, MacInnis BL, Hellman AB, Garrity PA, et al. Heat Avoidance Is Regulated by Transient Receptor Potential (TRP) Channels and a Neuropeptide Signaling Pathway in Caenorhabditis elegans. Genetics. 2011;188: 91–103. doi:10.1534/genetics.111.127100

72. Árnadóttir J, O'Hagan R, Chen Y, Goodman MB, Chalfie M. The DEG/ENaC Protein MEC-10 Regulates the Transduction Channel Complex in Caenorhabditis elegans Touch Receptor Neurons. J Neurosci. 2011;31: 12695–12704. doi:m

73. Chatzigeorgiou M, Grundy L, Kindt KS, Lee W-H, Driscoll M, Schafer WR. Spatial Asymmetry in the Mechanosensory Phenotypes of the C. elegans DEG/ENaC Gene mec-10. Journal of Neurophysiology. 2010;104: 3334–3344. doi:10.1152/jn.00330.2010

74. Kunitomo H, Sato H, Iwata R, Satoh Y, Ohno H, Yamada K, et al. Concentration memory-dependent synaptic plasticity of a taste circuit regulates salt concentration chemotaxis in Caenorhabditis elegans. Nat Commun. 2013;4: 2210. doi:10.1038/ncomms3210

75. Güiza J, Barría I, Sáez JC, Vega JL. Innexins: Expression, Regulation, and Functions. Frontiers in Physiology. 2018;9: 1414. doi:10.3389/fphys.2018.01414

76. Altun ZF, Chen B, Wang Z-W, Hall DH. High resolution map of Caenorhabditis elegans gap junction proteins. Developmental Dynamics. 2009;238: 1936–1950. doi:10.1002/dvdy.22025

769 77. Phelan P, Starich TA. Innexins get into the gap. BioEssays. 2001;23: 388–396. doi:10.1002/bies.1057

770 78. Taylor SR, Santpere G, Weinreb A, Barrett A, Reilly MB, Xu C, et al. Molecular topography of an entire nervous
771 system. Cell. 2021;184: 4329-4347.e23. doi:10.1016/j.cell.2021.06.023

772 79. Bhattacharya A, Aghayeva U, Berghoff E, Hobert O. Plasticity of the electrical connectome of C. elegans.
773 Neuroscience; 2018 Aug. doi:10.1101/406207

774 80. Tsukamoto S, Emmei T, Nakano S, Nishio N, Sasakura H, Mori I. The Caenorhabditis elegans INX-4/Innexin is
775 required for the fine-tuning of temperature orientation in thermotaxis behavior. Genes to Cells. 2020;25:
776 154–164. doi:10.1111/gtc.12745

777 81. Rabinowitch I, Upadhyaya B, Pant A, Galski D, Kreines L, Bai J. Circumventing neural damage in a C. elegans
778 chemosensory circuit using genetically engineered synapses. Cell Systems. 2021;12: 263-271.e4.
779 doi:10.1016/j.cels.2020.12.003

780 82. Choi M-K, Liu H, Wu T, Yang W, Zhang Y. NMDAR-mediated modulation of gap junction circuit regulates
781 olfactory learning in C. elegans. Nat Commun. 2020;11: 3467. doi:10.1038/s41467-020-17218-0

782 83. Rabinowitch I, Chatzigeorgiou M, Zhao B, Treinin M, Schafer WR. Rewiring neural circuits by the insertion of
783 ectopic electrical synapses in transgenic C. elegans. Nat Commun. 2014;5: 4442.
784 doi:10.1038/ncomms5442

785 84. Rabinowitch I, Schafer WR. Engineering new synaptic connections in the C. elegans connectome. Worm.
786 2015;4: e992668. doi:10.4161/21624054.2014.992668

787 85. Chang AJ, Chronis N, Karow DS, Marletta MA, Bargmann CI. A Distributed Chemosensory Circuit for Oxygen
788 Preference in C. elegans. PLOS Biology. 2006;4: e274. doi:10.1371/journal.pbio.0040274

789 86. Hart AC, Sims S, Kaplan JM. Synaptic code for sensory modalities revealed by C. elegans GLR-1 glutamate
790 receptor. Nature. 1995;378: 82–85. doi:10.1038/378082a0

791 87. Kaplan JM, Horvitz HR. A dual mechanosensory and chemosensory neuron in Caenorhabditis elegans.
792 Proceedings of the National Academy of Sciences. 1993;90: 2227–2231. doi:10.1073/pnas.90.6.2227

793 88. Yoshida K, Hirotsu T, Tagawa T, Oda S, Wakabayashi T, Iino Y, et al. Odour concentration-dependent olfactory
794 preference change in C. elegans. Nat Commun. 2012;3: 739. doi:10.1038/ncomms1750

795 89. Biron D, Wasserman S, Thomas JH, Samuel ADT, Sengupta P. An olfactory neuron responds stochastically to
796 temperature and modulates Caenorhabditis elegans thermotactic behavior. Proceedings of the National
797 Academy of Sciences. 2008;105: 11002–11007. doi:10.1073/pnas.0805004105

798 90. Kuhara A, Okumura M, Kimata T, Tanizawa Y, Takano R, Kimura KD, et al. Temperature Sensing by an
799 Olfactory Neuron in a Circuit Controlling Behavior of C. elegans. Science. 2008;320: 803–807.
800 doi:10.1126/science.1148922

801 91. Kano A, Matsuyama HJ, Nakano S, Mori I. AWC thermosensory neuron interferes with information
802 processing in a compact circuit regulating temperature-evoked posture dynamics in the nematode
803 *Caenorhabditis elegans*. Neuroscience Research. 2023;188: 10–27. doi:10.1016/j.neures.2022.11.001

804 92. O'Halloran DM, Altshuler-Keylin S, Zhang X-D, He C, Morales-Phan C, Yu Y, et al. Contribution of the cyclic
805 nucleotide gated channel subunit, CNG-3, to olfactory plasticity in Caenorhabditis elegans. Sci Rep. 2017;7.
806 doi:10.1038/s41598-017-00126-7

807 93. Peng C, Rich ED, Varnum MD. Subunit Configuration of Heteromeric Cone Cyclic Nucleotide-Gated
808 Channels. Neuron. 2004;42: 401–410. doi:10.1016/S0896-6273(04)00225-9

809 94. Shuart NG, Haitin Y, Camp SS, Black KD, Zagotta WN. Molecular mechanism for 3:1 subunit stoichiometry of
810 rod cyclic nucleotide-gated ion channels. Nat Commun. 2011;2: 457. doi:10.1038/ncomms1466

811 95. Zhong H, Molday LL, Molday RS, Yau K-W. The heteromeric cyclic nucleotide-gated channel adopts a 3A:1B
812 stoichiometry. Nature. 2002;420: 193–198. doi:10.1038/nature01201

813 96. Altanbadralt M, Basutta J, Hajen K, Parmar J, Sidhu BV. The effect of temperature on the speed of locomotion
814 in *Caenorhabditis elegans*. The Expedition. 2015;5. Available:
815 https://ojs.library.ubc.ca/index.php/expedition/article/view/188343

816 97. Parida L, Neogi S, Padmanabhan V. Effect of Temperature Pre-Exposure on the Locomotion and Chemotaxis
817 of C. elegans. PLOS ONE. 2014;9: e111342. doi:10.1371/journal.pone.0111342

818 98. Liu S, Schulze E, Baumeister R. Temperature- and Touch-Sensitive Neurons Couple CNG and TRPV Channel
819 Activities to Control Heat Avoidance in Caenorhabditis elegans. PLOS ONE. 2012;7: e32360.
820 doi:10.1371/journal.pone.0032360

821 99. Yuan C, Gerhards L, Solov'yov IA, Dedek K. Biotin-cGMP and -cAMP are able to permeate through the gap
822 junctions of some amacrine cells in the mouse retina despite their large size. Front Ophthalmol. 2024;3.
823 doi:10.3389/fopht.2023.1334602

824 100. Moore KB, Mitchell CK, Lin Y-P, Lee Y-H, Shihabeddin E, O'Brien J. Localized Calcium Signaling and the
825 Control of Coupling at Cx36 Gap Junctions. eNeuro. 2020;7. doi:10.1523/ENEURO.0445-19.2020

826 101. Vaughn MJ, Haas JS. On the Diverse Functions of Electrical Synapses. Front Cell Neurosci. 2022;16.
827 doi:10.3389/fncel.2022.910015

828 102. Jin EJ, Park S, Lyu X, Jin Y. Gap junctions: historical discoveries and new findings in the
829 Caenorhabditis elegans nervous system. Biology Open. 2020;9: bio053983. doi:10.1242/bio.053983

830 103. Brenner S. The genetics of Caenorhabditis elegans. Genetics. 1974;77: 71–94. doi:10.1093/genetics/77.1.71

831 104. Frøkjær-Jensen C, Davis MW, Ailion M, Jorgensen EM. Improved Mos1-mediated transgenesis in C. elegans.
832 Nat Methods. 2012;9: 117–118. doi:10.1038/nmeth.1865

833 105. Zhang L, Wang Y, Dong Y, Pant A, Liu Y, Masserman L, et al. The endophilin curvature-sensitive motif requires
834 electrostatic guidance to recycle synaptic vesicles in vivo. Developmental Cell. 2022;57: 750-766.e5.
835 doi:10.1016/j.devcel.2022.02.021

836 106. Coburn CM, Bargmann CI. A Putative Cyclic Nucleotide–Gated Channel Is Required for Sensory
837 Development and Function in C. elegans. Neuron. 1996;17: 695–706. doi:10.1016/S0896-6273(00)80201-9

838 107. Park J, Meisel JD, Kim DH. Immediate activation of chemosensory neuron gene expression by bacterial
839 metabolites is selectively induced by distinct cyclic GMP-dependent pathways in Caenorhabditis elegans.
840 PLoS Genet. 2020;16: e1008505. doi:10.1371/journal.pgen.1008505

841 108. Thompson O, Edgley M, Strasbourger P, Flibotte S, Ewing B, Adair R, et al. The million mutation project: A
842 new approach to genetics in Caenorhabditis elegans. Genome Res. 2013;23: 1749–1762.
843 doi:10.1101/gr.157651.113

844 109. Chalfie M, Sulston J. Developmental genetics of the mechanosensory neurons of Caenorhabditis elegans.
845 Developmental Biology. 1981;82: 358–370. doi:10.1016/0012-1606(81)90459-0

110. The C. elegans Deletion Mutant Consortium. Large-Scale Screening for Targeted Knockouts in the Caenorhabditis elegans Genome. G3 Genes|Genomes|Genetics. 2012;2: 1415–1425. doi:10.1534/g3.112.003830

111. Voelker L, Upadhyaya B, Ferkey DM, Woldemariam S, L'Etoile ND, Rabinowitch I, et al. INX-18 and INX-19 play distinct roles in electrical synapses that modulate aversive behavior in Caenorhabditis elegans. PLOS Genetics. 2019;15: e1008341. doi:10.1371/journal.pgen.1008341